ROYAL NORWEGIAN COUNCIL FOR SCIENTIFIC AND INDUSTRIAL RESEARCH

PROCEEDINGS FROM THE
SEMINAR ON

# SEISMOLOGY AND SEISMIC ARRAYS

OSLO, 22–25 NOVEMBER 1971

Editors: E S Husebye and H Bungum

Arranged in connection with the opening of The Norwegian Seismic Array (NORSAR) 1972

# INITIAL DISCRIMINATION RESULTS FROM THE NORWEGIAN SEISMIC ARRAY*

JOHN FILSON

Seismic Discrimination Group, Lincoln Laboratory,
42 Carleton Street, Cambridge, Massachusetts, USA

and

HILMAR BUNGUM

NTNT/NORSAR, P.O. Box 51, N-2007 Kjeller, Norway

## SUMMARY

A study has been made of the capability of the Norwegian Seismic Array to discriminate between earthquakes and underground explosions occurring in central Asia and western Russia. The ratio of surface to body wave magnitudes ($M_s$:$m_b$) has been used exclusively, the chief application of the array being in the detection and measurement of low amplitude surface waves. Beamforming and matched filtering were the signal enhancement techniques applied. Of 34 events in central Asia studied, 10 were identified as explosions, 22 earthquakes, and 2 were unidentifiable because of high, long period background noise. Five events in aseismic western Russia, all presumed to be explosions, showed wide variation in $M_s$:$m_b$; two of these measurements being close to the earthquake population of central Asia.

The $M_s$:$m_b$ measurements of central Asia explosions made in this and another study are compared with measurements of Nevada explosions. For a given $m_b$ the latter consistently have higher $M_s$ values. The possible causes of this are discussed and, depending on the cause, the array seems capable of detecting surface waves from an explosion of 4-16 kilotons yield at $40^{\circ}$ distance in central Asia. Strong seismic noise variations in Norway make this long period capability time dependent.

* This work was sponsored by the Advanced Research Projects Agency of the Department of Defense.

## INTRODUCTION

Since the spring of 1971 the completed Norwegian Seismic Array, NORSAR, has been operating in southeastern Norway. This installation offers the opportunity to apply certain array processing techniques to the problem of identification of earthquakes and explosions located in central Asia using a seismic array sited on the same continental land mass. This is a report of an initial study of the source discrimination capability of NORSAR.

In this study the sole discriminant applied was the ratio of surface wave to body wave magnitude ($M_s$:$m_b$). All of the events studied were reported by the National Ocean Survey (NOS) of the United States in the Preliminary Determination of Epicenters (PDE) and the values of $m_b$ and locations listed therein were accepted. Thus this study was reduced to one of detection and measurement of surface wave amplitudes, the computation of $M_s$, and the comparison of $M_s$:$m_b$ for presumed earthquakes and explosions.

## DETECTION AND MEASUREMENT OF SURFACE WAVES

At NORSAR 22 long period sites are evenly distributed around the circumference of two concentric rings; there is one center or "A" site. The outer or "C" ring is about 100 km in diameter containing 14 sites. The inner "B" ring is about 40 km in diameter with 7 sites. The long period instruments are in three component sets at each site, their response being narrowly peaked about 25 seconds period. The amplitude response of these instruments as a function of frequency is nominally the same as the long period instruments at the Large Aperture Seismic Array (LASA) (see Capon et al, 1969).

Only two rather elementary techniques of signal enhancement were used in this work, phased summation (beamforming) and cross-correlation using a reference waveform (matched filtering). Although other, more complex techniques exist, Capon et al (1969) found that the signal to noise ratio gain in long period seismic signals at an array, due to the series application of beamforming and matched filtering, was within about 3 db of optimum. Initially, when looking for signals too small to be seen on individual sensors, some groundwork must be laid before either of these techniques may be applied.

Considering beamforming first, when and how to form the beam given a weak signal must be determined from the group velocity from the source to the array, the phase velocity across the array, and an accurate location and origin time. Given that the location and origin time are known from the PDE lists only the phase and group velocities must be measured in order to apply the beamforming process. The group velocities of the fundamental mode Rayleigh wave from four central Asia events recorded at NORSAR were measured and are shown in Fig 1. Although there is some scatter in the measurements, a clear minimum exists near 18 seconds period, typical of continental paths, and the group velocity at 20 seconds is taken to be 3.0 km/sec. Since the measurement of $M_s$ will ultimately be made at or near 20 seconds period, recordings of that period are of particular interest.

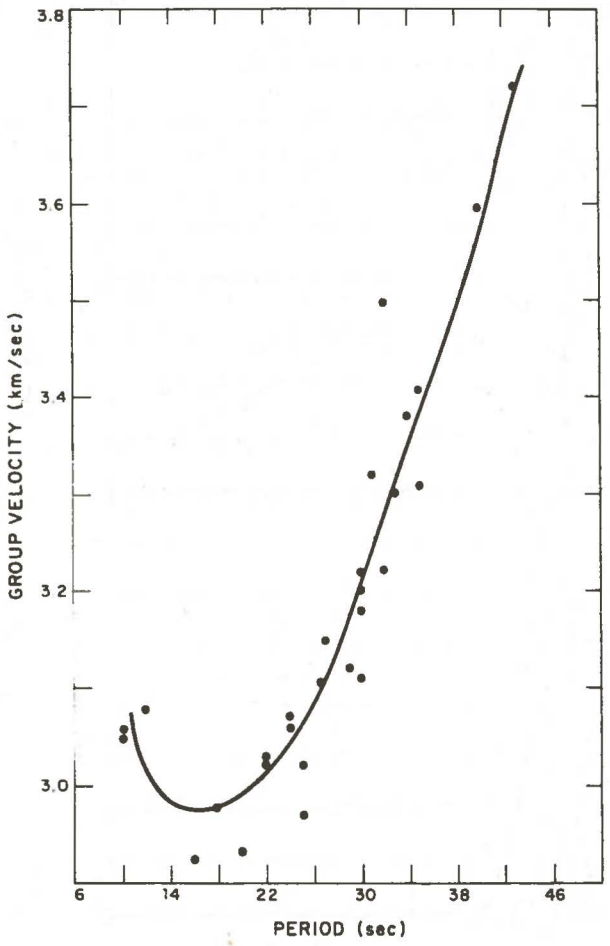


Fig 1. Rayleigh wave group velocity measurements at NORSAR from 4 events in central Asia.

Phase velocities across NORSAR were measured using the high resolution, frequency-wavenumber analysis of Capon (1969). Although there was considerable scatter a velocity of 3.5 km/sec represents an average of the Rayleigh wave phase velocity measurements at 20 seconds. The high resolution technique also yields a direction of approach which was found to be within $10^{\circ}$ of the computed great circle azimuth at periods between 10 and 50 seconds. Based on these observations, delays computed using 3.5 km/sec and the great circle azimuth from the NOS location were used in beamforming.

Once the beam is formed the question of signal deterioration due to beamforming must be addressed. In order to do this the following experiment was performed. For a given event with high signal to noise ratio the

beam was formed using the long period vertical sensors and the parameters given above and its power spectrum computed. Then the average spectrum was computed using the 14 individual sensors of the outer C ring. The difference between the beam and average spectrum is then computed as a function of frequency. Data used in such an experiment are shown in Fig 2 where the long period vertical recordings for an event to the east northeast at 40° distance are displayed. The individual channels have been aligned and the aligned sum or beam displayed in the top trace in place of 01A. The characteristic nature of the Rayleigh wave of events from this region can be seen in Fig 2.

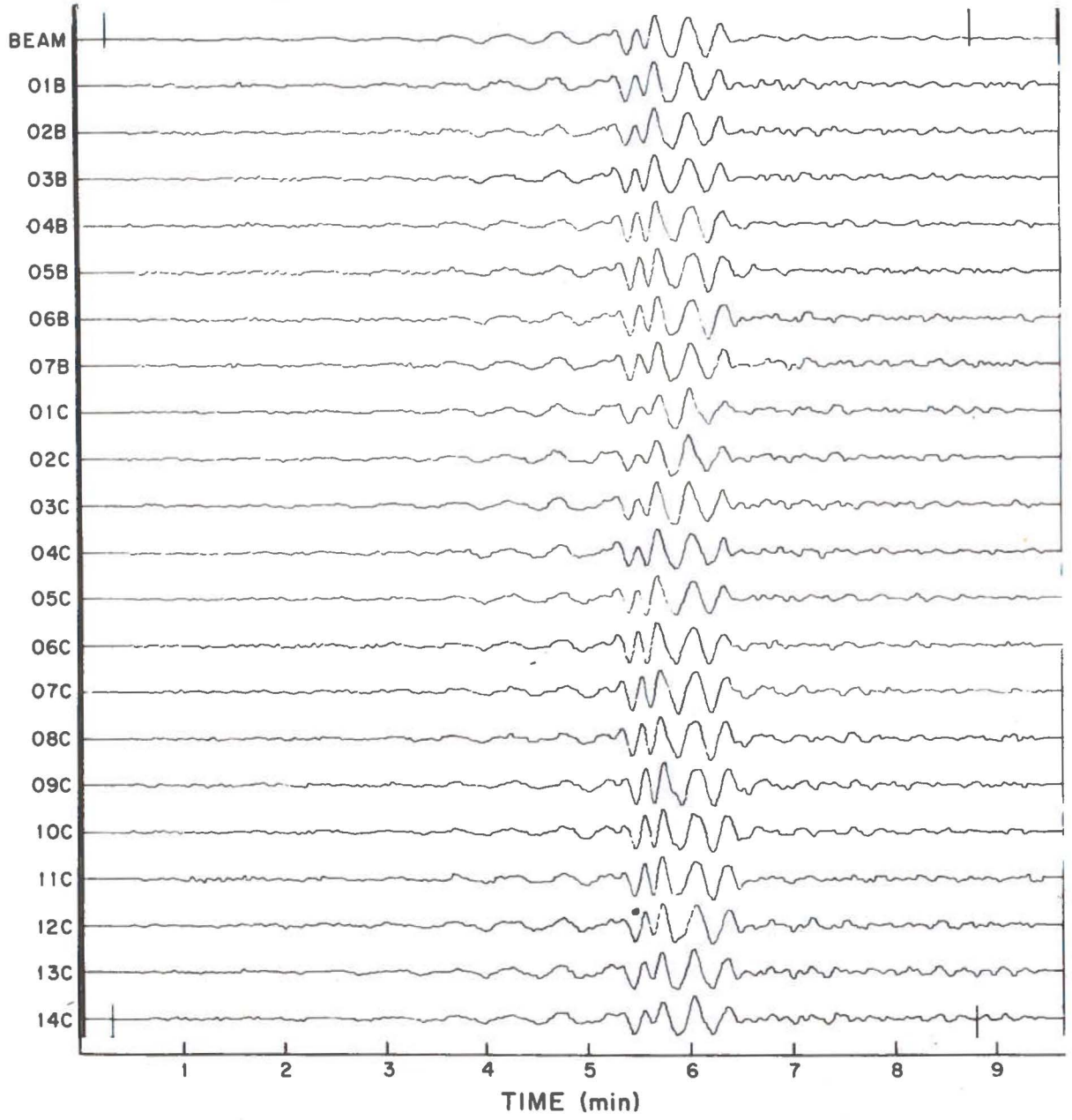


Fig 2. Beam and aligned traces of long period vertical component of recorded Rayleigh wave motion from eastern Kazakh event of 25 April 1971.

The traces begin with long period motion of about 40 seconds period, this is followed by relatively shorter periods near 15 seconds, the

traces ending with motion near 20 seconds period. This 20 second motion is usually the largest of events at this distance which facilitates the application of $M_s$ formulae based on motion of that period. In Fig 3a the power spectrum of the beam or top trace of Fig 2 is compared to average power spectrum computed using the 14 C ring sensors. In Fig 3b the difference between these two spectra is plotted versus frequency. It is seen that at 20 seconds period the

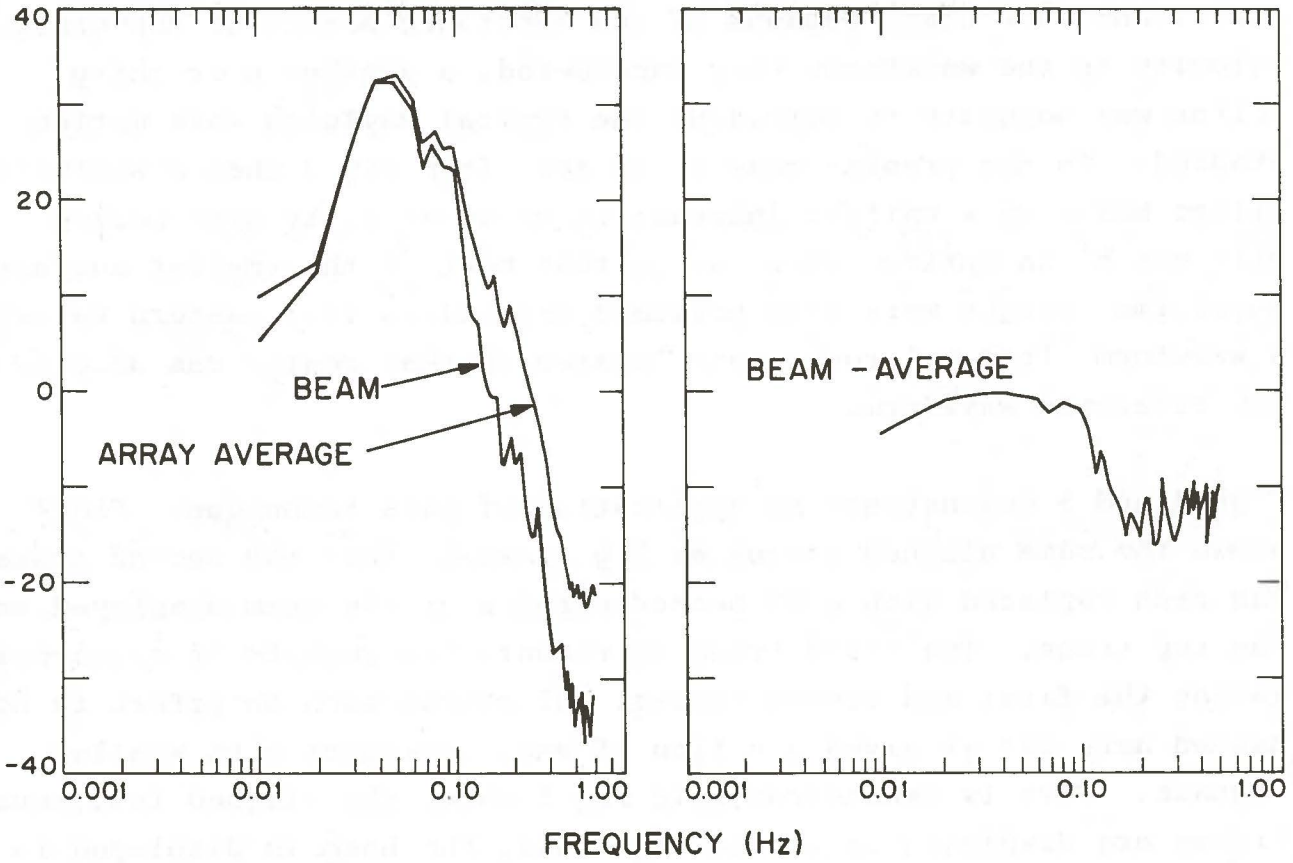


Fig 3a. Power spectrum of the beam of Fig 2 and the array average power spectrum computed using traces 1C-14C of Fig 2. Power is measured in decibels relative to 1 $m_\mu{}^2$/Hz at 20 seconds.

Fig 3b. The difference between the beam and array average spectrum of Fig 3a.

beam is about 2 db below the average spectrum. At periods less than 10 seconds the beam spectrum ranges from 10 to 15 db below the average spectrum. In the case of incoherent noise a signal to noise ratio increase of 20 log $\sqrt{22}\simeq 13$ db would be expected. In any case the beam loss of 2 db at 20 seconds was verified using another event from the same location as that of Figs 2 and 3 and a correction of +.1 units has been applied to all $M_s$ measurements made from the beam.

The second signal processing technique applied makes use of a reference waveform or matched filter technique. In this technique an attempt is made to verify the existence of a distinctive waveform in a trace with low signal to noise ratio through the cross-correlation of that trace with a noise free approximation of the sought for signal. Capon et al (1969) discuss the technique in detail and show that, because of the monotonic nature of the group velocity in the waveforms they considered, a synthetic or chirp filter was adequate to represent the typical Rayleigh wave motion studied. In the present case it is seen from Fig 2 that a synthetic filter based on a uniform increase in group velocity with period will not be an optimum one. Given that most of the smaller surface waveforms sought were from presumed explosions from eastern Kazakh, a waveform from a larger event located in that region was adopted as the reference waveform.

Figs 4 and 5 demonstrate an application of this technique. Fig 4 shows the same aligned traces as Fig 2 except that the second trace has been replaced with a 90 second portion of the beam displayed on the top trace. The third trace represents the results of cross-correlating the first and second traces. Of course such an effort is not needed here but it gives a notion of what to expect with smaller signals. This is demonstrated in Fig 5 where the aligned individual traces are displayed in the lower traces, the beam is displayed in the top trace, the reference waveform of Fig 4 is displayed in the second trace and the third trace is the result of cross-correlating the top two traces. The data displayed in Fig 4 and 5 are delayed at equal intervals following the origin time. Although there is a suggestion of an arrival at the appropriate time on the beam (top trace) of Fig 5 one feels much more confident of this arrival when the results of cross-correlation (third trace) are considered.

In practice a longer (180 second) segment of the beam of Fig 4 was used as the reference waveform to include the longer period, earlier portion of the wavetrain. However, because of the low amplitude nature of this motion the increase in the amplitude of the cross-correlation peak was only about 10%. In the example of Fig 5 the increase in the signal to noise ratio is about 6 db as it was when the longer reference trace was applied to the same data. This would imply that the effective band-

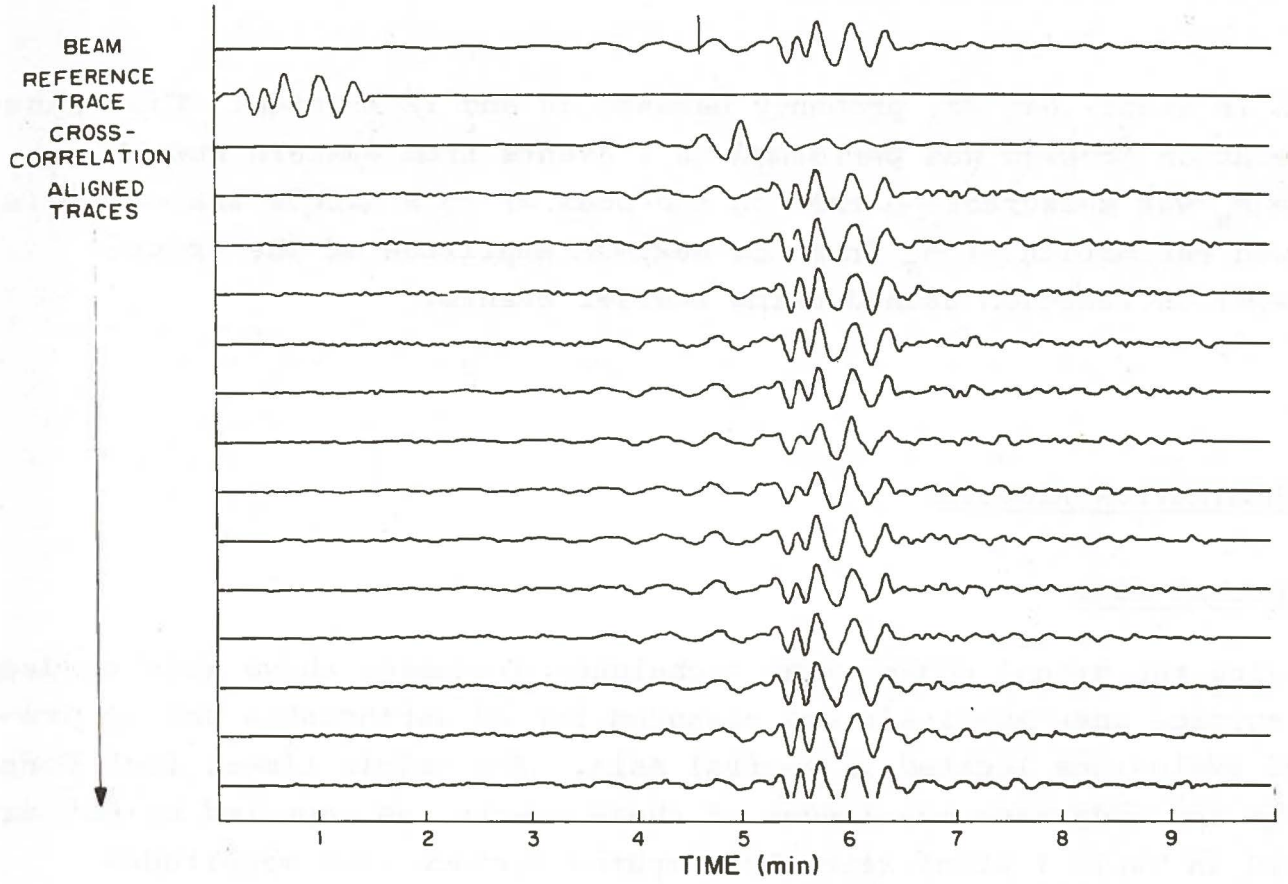


Fig 4. Rayleigh wave beam of event of 25 April 1971; reference waveform from 90-second portion of this beam; and the cross-correlation of the reference trace and beam.

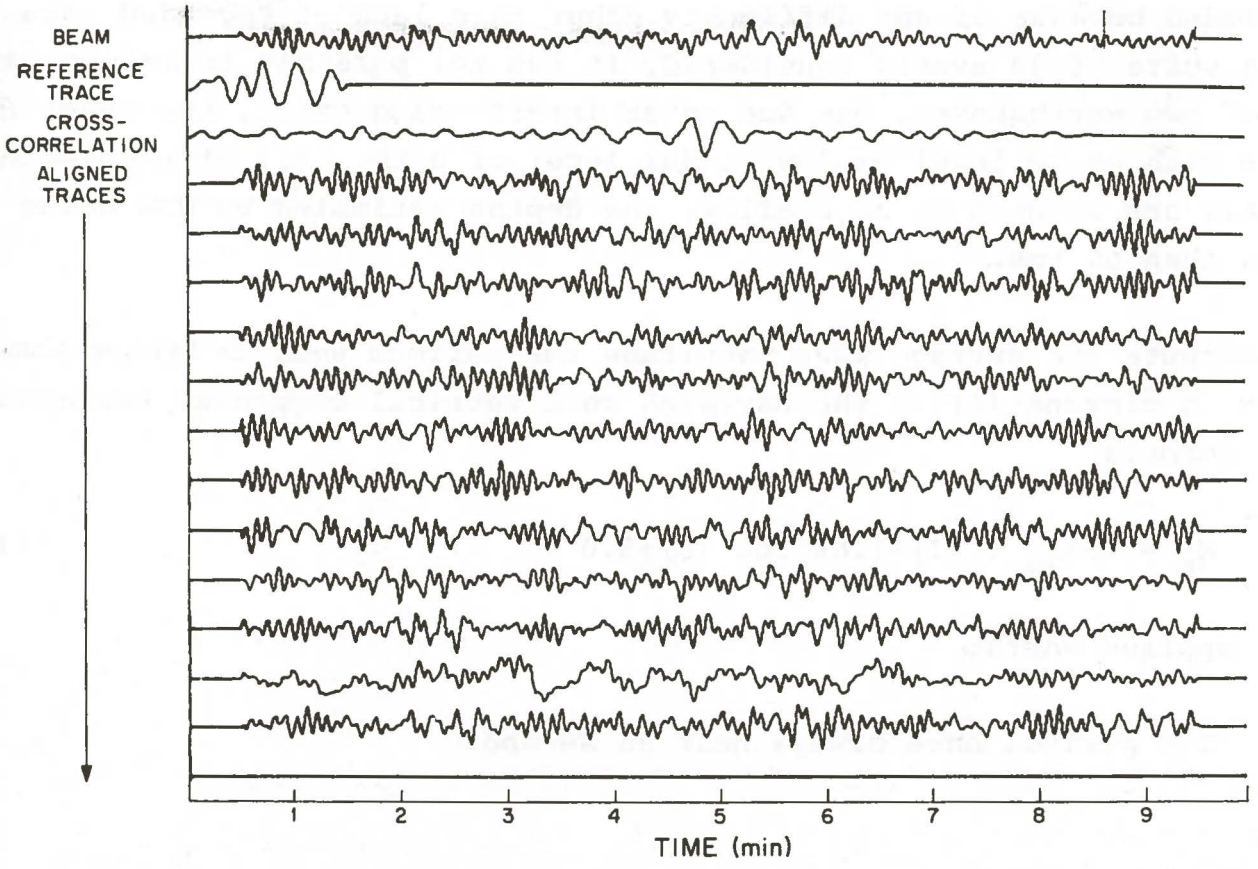


Fig 5. Rayleigh wave beam of event from eastern Kazakh on 9 Oct 1971, reference waveform from event of Fig 4, and cross-correlation of the reference trace and beam.

width is about .045 Hz, probably between 30 and 12 seconds. The cross-correlation process was performed on 4 events from eastern Kazakh where $M_s$ was measurable either on the beam or on a single trace. This allowed estimation of $M_s$ from the maximum amplitude of the cross-correlation function gained using smaller events.

## DISCRIMINATION RESULTS

### Central Asia

Applying the signal enhancement techniques discussed above when needed, the surface wave magnitude was measured for 22 earthquakes and 10 presumed explosions located in central Asia. The origin times, locations, depths and body wave magnitudes of these events, as reported by NOS are listed in Table I along with the computed surface wave magnitudes. This list is not comprehensive in that it does not include all of the events that occurred during the time period studied. Nor is it selective in that no region was avoided or no event once considered was excluded because of any difficulty other than lack of recorded data. In this suite of 34 events considered, it was not possible to measure the $M_s$ of two earthquakes, one due to an interferring event, the other due to a high noise level or low signal level or both. All of the earthquakes are assumed to be shallow, the depths estimated by NOS being less than 50 kms.

To compute the surface wave magnitude the maximum peak to trough amplitude in microns (A) of the Rayleigh wave vertical component was measured. The formula

$$M_s = \log_{10} (A/T) + 1.66 \log (\Delta) + 3.0 \qquad (1)$$

was applied where:

T = period, here always near 20 seconds

and

$\Delta$ = distance in central angle degrees.

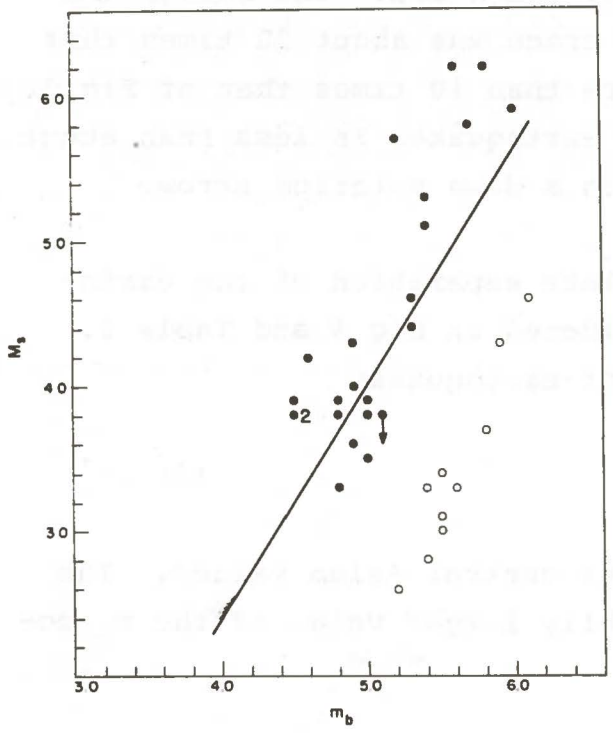


Fig 6. NORSAR $M_s$ versus NOS $m_b$, for central Asia earthquakes (closed circles) and presumed explosions (open circles). The straight line is the Gutenberg-Richter relation of equation (2).

An additional +.1 $M_s$ unit was applied when A was measured on the array beam. In Fig 6 the measured $M_s$ is plotted versus the NOS $m_b$ value.

The smallest $M_s$ reported in Table I is 2.6 for the eastern Kazakh explosion of May 25, 1971. A display of the individual traces and the array beam of this event is shown in Fig 7. Although the signal is not obvious on any individual trace the authors feel it can be measured with some confidence on the array beam. The $M_s$ of the Kirgiz event of Feb 21, 1971 ($m_b$ = 4.2) could not be measured due to a low signal level with respect to the interferring Rayleigh waves from a large ($m_b$ = 6.3, 6.8 (PAS)) event occuring one hour previously near the Chile-Argentina border. This event is not plotted on

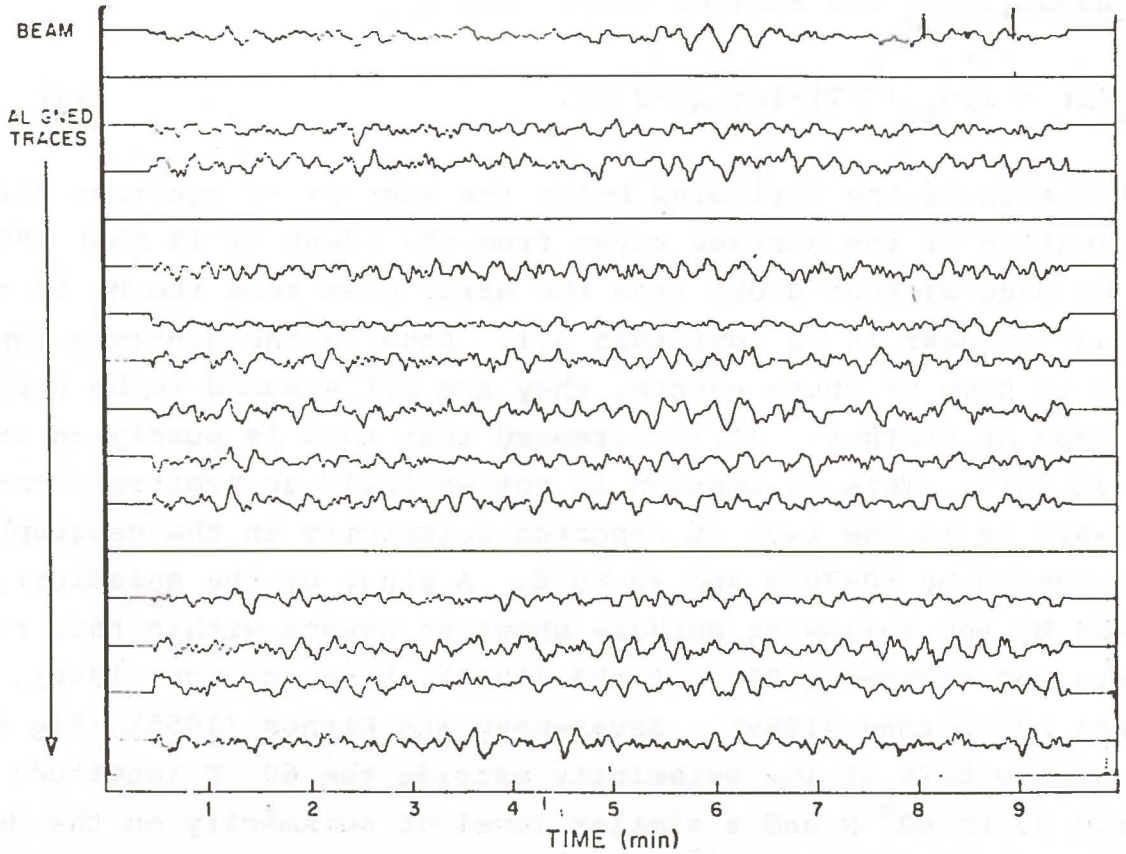


Fig 7. Beam and aligned traces of eastern Kazakh event of 25 May 1971. The $M_s$ of 2.6 was the smallest measured for any event of this study.

Fig 8. $M_s$ could not be measured for the Tibet event of Oct 24, 1971 due to a low signal level with respect to the noise. The background noise at NORSAR on this day on a single trace was about 20 times that seen in Fig 7, the noise on the beam more than 10 times that of Fig 7. The $M_s$ of this event, presumed to be an earthquake, is less than about 3.8. This event is plotted on Fig 8 with a down pointing arrow.

With these two exceptions there is complete separation of the earthquakes and the presumed explosions considered in Fig 6 and Table I. The Gutenberg-Richter (1956) relation for earthquakes

$$M_s = 1.59\ m_b - 3.97 \qquad (2)$$

is drawn on Fig 6 for comparison with the central Asian values. The earthquake data of Fig 6 suggest a slightly larger value of the $m_b$ coefficient in (2) for this region.

Western Russia

Five events from western Russia were included in this study, the NOS parameters and the $M_s$ values measured at NORSAR being given in Table II. Because of the proximity of these events to the array the $M_s$ formula of Evernden (1971) was applied where

$$M_s(E) = \log_{10}(A/T) + \log_{10}\Delta + 3.92, \qquad (3)$$

the definition of the variables being the same as in equation (1). The identification of the surface waves from the event of 19 Sept 1971 cannot be made without doubt from the array beam thus the $M_s$ of this event must be near to or less than 3.1. Despite the non-zero depths assigned to some of these events, they are all assumed to be explosions of one type or another. It is stressed that this is purely an assumption of the authors. This assumption is not entirely an arbitrary one, its chief basis is in the lack of reported seismicity in the geographical region bounded by 50-70°N and 40-60°E. A study of the seismicity maps published by the following authors shows no events within this region: Gutenberg and Richter (1954), Rothé (1969), Lang and Sun (1966), and Barazangi and Dorman (1969). Savarensky and Kirnos (1955) (Fig 60) show a narrow belt of low seismicity astride the 60° E longitude running from 53 to 60° N and a similar level of seismicity on the Murmansk peninsula. Savarensky, et al (1962) show 4 events, magnitude less than

5 1/4, occurring between 1914 - 1957 and located in the vicinity of 60 N - 60 E. The conclusion based on this brief survey of seismicity information is that western Russia is essentially aseismic with the possibility of infrequent events of magnitude less than 5.5 in the mid-Urals and on and just south of the Murmansk peninsula.

These seismicity conditions make any regional discrimination experiment impossible since there does not exist a large number of earthquakes against which to test the presumed explosions. Furthermore the apparent lack of regional seismicity, the shallow depths assigned by NOS, and the origin times all within seven seconds of an hour force us to assume that all of the events of Table II are explosions. In Fig 8 we have plotted NOS $m_b$ versus $M_s$ computed using (3) for these five events. The Gutenberg-Richter earthquake relation is also drawn on this figure. Here the trend in the $M_s$-$m_b$ relation for explosions is not as well defined as it is for the central Asian data of Fig 6. In addition to this scatter, two of the points would be identified as earthquakes if the Gutenberg-Richter line was used in lieu of a significant earthquake population. Given the above assumptions we arrive at the conclusion that the presumed explosions in western Russia are detonated under varying physical conditions and that their primary purpose differs from that of the presumed explosions in eastern Kazakh.

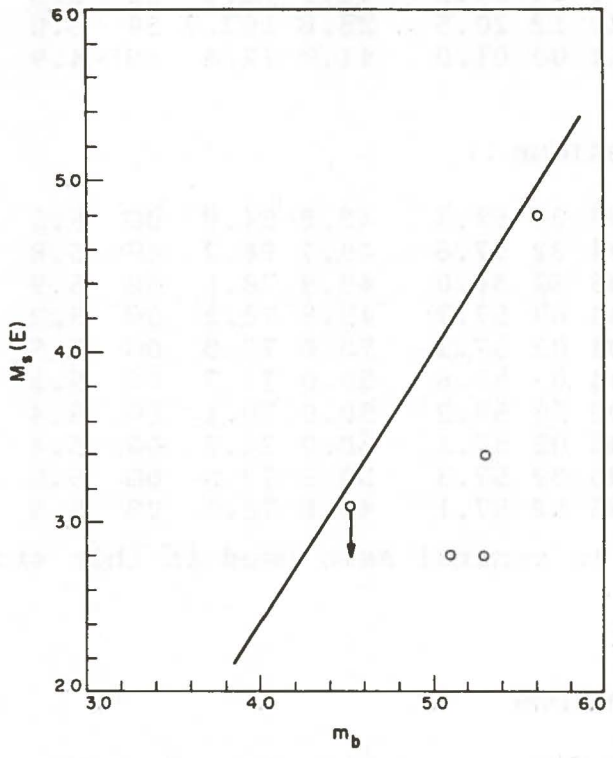


Fig 8. NORSAR $M_S$ (computed using equation (3))versus NOS $m_b$ for western Russia events all presumed to be explosions. The straight line is the Gutenberg-Richter relation.

TABLE I

PRESUMED EARTHQUAKES

| Date | Region | O Time | Lat | Lon | H | MB | MS |
|---|---|---|---|---|---|---|---|
| 21 Feb 71 | Kirgiz | 11 45 24.8 | 40.8 | 72.6 | N | 4.2 | -- |
| 1 Mar 71 | Tsinghai China | 00 56 51.5 | 34.1 | 95.8 | N | 4.6 | 4.2 |
| 23 Mar 71 | Kirgiz Sinkiang Border | 09 52 12.3 | 41.5 | 79.3 | N | 5.7 | 5.8 |
| 23 Mar 71 | Kirgiz Sinkiang Border | 20 47 17.4 | 41.5 | 79.3 | N | 6.0 | 5.9 |
| 24 Mar 71 | Tsinghai China | 13 54 17.7 | 35.5 | 98.2 | 12 | 5.8 | 6.2 |
| 24 Mar 71 | Kirgiz Sinkiang | 20 54 28.6 | 41.5 | 79.5 | 18 | 5.3 | 4.4 |
| 24 Mar 71 | Kirgiz Sinkiang | 21 01 54.9 | 41.4 | 79.4 | 25 | 5.3 | 4.6 |
| 31 Mar 71 | Southern Sinkiang | 20 00 31.5 | 39.6 | 74.8 | 38 | 4.8 | 3.3 |
| 4 Apr 71 | Tadzhik Sinkiang | 01 35 23.3 | 38.4 | 73.3 | N | 4.8 | 3.8 |
| 6 Apr 71 | Southern Sinkiang | 03 02 57.0 | 39.6 | 77.8 | N | 4.5 | 3.8 |
| 18 Apr 71 | Tadzhik | 07 24 14.3 | 39.1 | 71.7 | N | 4.5 | 3.8 |
| 3 May 71 | Tibet | 00 33 22.5 | 30.8 | 84.5 | 16 | 5.4 | 5.1 |
| 22 May 71 | Tibet | 20 03 32.4 | 32.4 | 92.1 | N | 5.6 | 6.2 |
| 27 May 71 | Tadzhik | 00 30 27.7 | 38.3 | 69.0 | 36 | 4.8 | 3.9 |
| 4 Jun 71 | Tibet | 14 10 46.0 | 32.2 | 95.2 | N | 5.0 | 3.5 |
| 4 Jun 71 | Tibet | 20 49 58.3 | 32.2 | 92.1 | N | 5.0 | 3.8 |
| 3 Jul 71 | Kirgiz Sinkiang | 04 26 22.1 | 41.3 | 79.3 | 17 | 4.9 | 3.6 |
| 30 Jul 71 | Kirgiz Sinkiang | 20 13 1..1 | 41.3 | 79.3 | N | 4.5 | 3.9 |
| 24 Aug 71 | Central Russia | 16 33 22.7 | 52.2 | 91.4 | N | 5.2 | 5.7 |
| 1 Oct 71 | Tadzhik | 16 27 47.7 | 38.6 | 69.8 | 36 | 4.9 | 4.3 |
| 24 Oct 71 | Tibet | 08 59 04.6 | 28.2 | 87.2 | 44 | 5.1 | 3.8 |
| 28 Oct 71 | Kirgiz Sinkiang | 13 50 57.1 | 41.9 | 72.4 | 22 | 5.5 | 5.3 |
| 4 Nov 71 | Szechwan China | 20 12 20.5 | 28.8 | 103.7 | 34 | 5.0 | 3.9 |
| 19 Nov 71 | Central Kazakh | 01 00 01.0 | 41.9 | 72.4 | N | 4.9 | 4.0 |

PRESUMED EXPLOSIONS

| | | | | | | | |
|---|---|---|---|---|---|---|---|
| 23 Dec 70 | Western Kazakh | 07 00 57.3 | 43.8 | 54.8 | 0G | 6.1 | 4.6 |
| 22 Mar 71 | Eastern Kazakh | 04 32 57.8 | 49.7 | 78.2 | 0G | 5.8 | 3.7 |
| 25 Apr 71 | Eastern Kazakh | 03 32 58.0 | 49.8 | 78.1 | 0G | 5.9 | 4.3 |
| 25 May 71 | Eastern Kazakh | 04 02 57.7 | 49.8 | 78.2 | 0G | 5.2 | 2.6 |
| 6 Jun 71 | Eastern Kazakh | 04 02 57.1 | 50.0 | 77.8 | 0G | 5.5 | 3.0 |
| 19 Jun 71 | Eastern Kazakh | 04 03 57.6 | 50.0 | 77.7 | 0G | 5.5 | 3.1 |
| 30 Jun 71 | Eastern Kazakh | 03 56 57.2 | 50.0 | 79.1 | 0G | 5.4 | 3.3 |
| 9 Oct 71 | Eastern Kazakh | 06 02 57.1 | 50.0 | 77.7 | 0G | 5.4 | 2.8 |
| 21 Oct 71 | Eastern Kazakh | 06 02 57.3 | 50.5 | 77.6 | 0G | 5.6 | 3.3 |
| 29 Nov 71 | Eastern Kazakh | 06 02 57.1 | 49.8 | 78.1 | 0G | 5.5 | 3.4 |

Presumed explosions and earthquakes in central Asia used in this study.

TABLE II

PRESUMED EXPLOSIONS

| Date | Region | O Time | Lat | Lon | H | MB | MS |
|---|---|---|---|---|---|---|---|
| 23 Mar 71 | Ural Mountains | 06 59 56.0 | 61.3 | 56.5 | 0G | 5.6 | 4.8 |
| 10 Jul 71 | Ural Mountains | 16 59 59.3 | 64.2 | 55.2 | 0G | 5.3 | 2.8 |
| 19 Sep 71 | Western Russia | 11 00 06.8 | 57.8 | 41.1 | N | 4.5 | 3.1 |
| 4 Oct 71 | Western Russia | 10 00 02.0 | 61.6 | 47.1 | 13 | 5.1 | 2.8 |
| 22 Oct 71 | Western Russia | 05 00 00.4 | 51.6 | 54.5 | 6 | 5.3 | 3.4 |

Presumed explosions in western Russia used in this study.

## DISCUSSION

There are three points which have arisen in this study which we consider significant. Firstly, severe microseismic storms make the long period detection capability of NORSAR time dependent. The amplitude of the microseisms was found to vary by a factor of 20 in this study. Although this variation is probably seasonal and possibly predictable, it will have to be studied over an extended time period before comprehensive statements can be made concerning the operational discrimination capability of NORSAR.

Secondly, Fig 9 shows that the located detection capability of NOS in central Asia has a lower limit of about 4.5 while the surface wave detection capability of NORSAR extends somewhat below $M_s = 3.0$ for that same region. Thus in addition to the study of seasonal noise variation, other means of gaining reliable event locations in central Asia must be used or developed in the determination of NORSAR's discrimination capability.

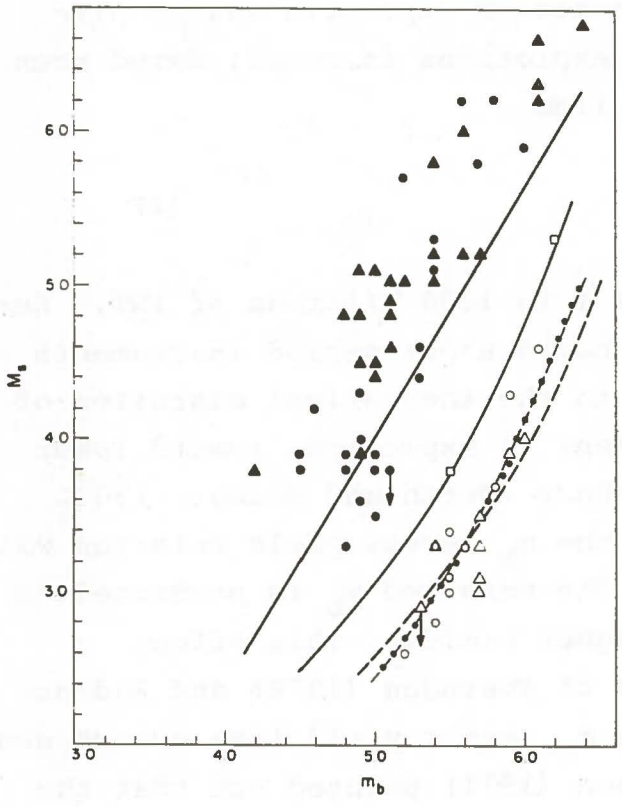


Fig 9. Combined NORSAR (o) LASA (Δ) $M_s$ versus NOS $m_b$ for central Asia earthquakes (closed symbols) and presumed explosions (open synbols). The straight line is again equation (2), the curved solid line is the Evernden et al (1971) line for NTS, the dashed line is the NTS line shifted .4 $m_b$ units to the right, the dotted line is the NTS line shifted .6 $M_s$ units downward. The open squares are NTS explosion $M_s$ values at NORSAR versus NOS $m_b$.

Thirdly, we would like to elaborate on the suite of $M_s$:$m_b$ values of presumed explosions in central Asia and attempt to discuss the NORSAR surface wave detection capability for that region in terms of source size. Compared with similar measurements of explosions at the United States' Nevada Test Site (NTS), for a given $m_b$ the $M_s$ values of Fig 6 appear low. In order to test for a systematic error we have plotted as triangles in Fig 9 (after applying a correction for a slight difference in the method of calculating $M_s$) $M_s$ values of central Asia events measured by Capon et al (1969) versus NOS $m_b$. Also plotted as circles in Fig 9 are the NORSAR data of Fig 6. In Fig 9 no systematic difference in $M_s$:$m_b$ measurements of either earthquakes or explosions is seen between the two data sources.

Also in Fig 9, plotted as a solid curved line, is the NTS $M_s$:$m_b$ relation of Evernden et al (1971) which is based on the measurements of 20 second surface waves and the same $m_b$ calculation as used by NOS or, for $\Delta<20^{\circ}$, an equivalent procedure developed by Evernden (1967). NORSAR $M_s$ versus NOS $m_b$ values for 2 NTS explosions are plotted as open squares on Fig 9. Since these values lie on or near Evernden's line they give some assurance that this line may be a fair representation of NTS $M_s$:$m_b$ at NORSAR. Most of the central Asia points lie from .1 to .6 $m_b$ units to the right of or about .1 to .6 $M_s$ units below the NTS line. The question then is: Are these differences due to variation of the $m_b$ or $M_s$ values measured from the two source sites?

Various authors, most recently Marshall et al (1971), have set forth evidence that $M_s$ is a more stable estimate of explosive source size or yield than $m_b$. They show that for explosions in consilidated rock most $M_s$ observations lie close to the line

$$M_s = \log Y + 2.0 \qquad (4)$$

where Y represents yields ranging from 4 to 1300 kilotons of TNT. Because of the limited band width of standard short period instruments used in the measurement of $m_b$ and due to the theoretical migration of the peak frequency of ground displacement of explosions toward lower frequencies with increase in yield, others (Werth and Herbst, 1963; Carpenter, 1967) have predicted that the $m_b$ versus yield relation will not be a linear one over all yields. The measured $m_b$ is predicted to increase less rapidly with yield at higher yields. This effect appears to be identifiable on the data of Evernden (1970) and Rodean (1971). In both cases the bend in the $m_b$ versus yield line occurs near 100 kilotons yield. Evernden and Filson (1971) pointed out that the combination of linear $M_s$:yield dependence and an $m_b$:yield relation described above would give rise to an $M_s$:$m_b$ dependence for explosions of the nature shown by the curved solid line in Fig 9.

In Fig 9 both the NTS line and the central Asia explosion data show a change in slope between $M_s$ = 3 and $M_s$ = 4. The dashed line through the central Asia points in Fig 9 is simply the NTS line displaced .4 units to the right. The dotted line through the central Asia points is the NTS line displace .6 $M_s$ units downward. Although not conclusive, the latter gives a slightly better representation of the data supporting the notion that at a given yield the $M_s$ values from central Asia explosions are low compared to NTS.

Ward and Toksöz (1970) and Evernden and Clark (1970) have attributed low $m_b$ values measured in the western United States to relatively higher P wave attenuation in the upper mantle beneath this region. The former assert that $m_b$ values measured at LASA should be .4 units lower than those at NORSAR based on a higher Q model for the upper mantle beneath NORSAR. Assuming attenuation of the form exp $(-\pi f t^*)$ Filson (1970) estimated the value of $t^*$ from central Asia explosions to Norway to be .05 by spectral fitting over the band f = .6 - 3.0 HZ. Frasier (1971) estimated the value of $t^*$ from NTS to Norway to be .4 by matching the explosion waveform in the time domain. At 1.0 Hz these variations in $t^*$ would imply a difference of nearly .4 units $m_b$ for explosions of the same yield detonated at the two sites under similar conditions and recorded in Norway. This assumes $m_b$ is computed using a world average depth-distance correction. Because the upper mantle paths of P waves from NTS and central Asia are essentially the same beneath Norway, it seems reasonable to attribute the attenuation contrasts to the source region, again suggesting higher attenuation under the western United States.

Thus the recognized stability of the dependence of $M_s$ upon yield and the evidence for greater short period attenuation beneath the western United States supports the argument that the differences between the NTS and central Asia data of Fig 9 is due to variation in $m_b$ not $M_s$. If this assertion concerning $m_b$ is valid, then, using (4), we are able to estimate the detection capability of NORSAR in terms of yield. In the case of the traces shown in Fig 7, we conclude that using beam-forming one can, on occasion, detect and measure surface waves from an event $40^\circ$ distance in central Asia of a size equivalent of 4 kilotons of TNT in hard rock. If, on the other hand, equation (4) (which is based primarily on NTS data) is not generally valid for central Asia and the $m_b$ measurements from explosions at the two sites are directly comparable then the data of Fig 7 may result from an explosion equivalent to one of $M_s$ = 3.2 or 16 kilotons yield at NTS. Presently, neither of these numbers should be considered an operational capability because of the strong amplitude variation with time of the noise field at NORSAR.

ACKNOWLEDGEMENT

This work was performed during a two month period at the NORSAR Data Processing Center near Kjeller, Norway. One of us, J.F., expresses

his gratitude to the Royal Norwegian Council for Scientific and Industrial Research and the staff at Kjeller for their kind support and forbearance during that period.

REFERENCES

1. M. Barazangi and J. Dorman: World seismicity maps compiled from ESSA Coast and Geodetic Survey epicenter data 1961-1967, Bull. seism. Soc. Am., 59, 369-380, 1969.

2. J. Capon: High resolution frequency-wavenumber spectrum analysis, Proceedings of the IEEE, 57, 1408-1418, 1969.

3. J. Capon, R.J. Greenfield and R.T. Lacoss: Long period signal processing results for the large aperture seismic array, Geophysics, 34, 305-329, 1969.

4. E.W. Carpenter: Teleseismic signals calculated for underground, underwater, and atmospheric explosions, Geophysics, 32, 17-32, 1967.

5. J.F. Evernden: Magnitude determination at regional and near-regional distances in the United States, Bull. seis. Soc. Am., 57, 591-639, 1967.

6. J.F. Evernden: Magnitude versus yields of explosions, J. geophys. Res., 75, 1028-1032, 1970.

7. J.F. Evernden and D.M. Clark: Study of teleseismic P II-Amplitude data, Physics of the Earth and Planetary Interiors, 4, 24-31, 1970.

8. J.F. Evernden: Variation of Rayleigh wave amplitude with distance, Bull. seism. Soc. Am., 61, 231-240, 1971.

9. J.F. Evernden and J. Filson: Regional dependence of surface-wave versus body wave magnitudes, J. geophys. Res., 76, 3303-3308, 1971.

10. J.F. Evernden, W.J. Best, P.W. Pomeroy, T.V. McEvilly, J.M. Savino, and L.R. Sykes: Discrimination between small-magnitude earthquakes and explosions, J. geophys. Res., 76, 8042-8055, 1971.

11. J. Filson: On estimating explosive source parameters at teleseismic distances, MIT Lincoln Laboratory Technical Note 1970-9, 1970.

12. C.W. Frasier: Prediction of teleseismic P shapes from explosions, MIT Lincoln Laboratory Semiannual Technical Summary 30 June, 6-7, 1971.

13. B. Gutenberg and C.F. Richter: Seismicity of the earth and associated phenomena, Hafner Publishing Co., New York and London, 1954.

14. B. Gutenberg and C.F. Richter: Magnitude and energy of earthquakes, Ann. di Geofis., 9, 1-15, 1956.

15. W.J. Lang and R.J. Sun: Atlas of the Sino-Soviet block to support detection of underground nuclear testing, United States Geological Survey, Washington D.C., 1966.

16. P.D. Marshall, A. Douglas, and J.A. Hudson: Surface waves from underground explosions, Nature, 234, 8-9, 1971.

17. H.C. Rodean: Nuclear-explosion seismology, United States Atomic Energy Commission Division of Technical Information, TID-25572, 1971.

18. J.P. Rothe: The seismicity of the earth 1953-1965, United Nations Educational, Scientific and Cultural Organization, Paris, 1969.

19. E.F. Savarensky and D.P. Kirnos: Elementi Seysmologie i Seysmometrii (Elements of Seismology and Seismometry) State Publishing House of Technical-Theoretical Literature, Moscow, 1955.

20. E.F. Savarensky, S.L. Soloviev, D.A. Khardin (eds.): Atlas Zemletriasenii v SSSR (Atlas of the Seismicity of the USSR), Akad. Nauk. SSSR, Moscow, 1962.

21. R.W. Ward and M.N. Toksöz: Causes of regional variation of magnitudes, Bull. seism. Soc. Am., 61, 649-670, 1971.

22. G.C. Werth and R.F. Herbst: Comparison of the amplitude of seismic waves from nuclear explosions in four mediums, J. geophys. Res., 68, 1463-1475, 1963.